Journal of the European Ceramic Society **11** (1993) 219–230

Diffusional Phenomena Related to Implantation of ^{13}C Ions in SiC

P. Eveno

Laboratoire de Physique des Matériaux, CNRS Bellevue, 1 Place Aristide Briand, 92195 Meudon Cedex, France

J. Li,* A. M. Huntz

Laboratoire de Métallurgie Structurale, ISMA, CNRS URA 1107, Université Paris XI, 91405 Orsay, France

&

J. Chaumont

CSNSM, Laboratoire CNRS, Université Paris XI, 91405 Orsay, France

(Received 4 October 1991; revised version received 15 May 1992; accepted 11 August 1992)

Abstract

The effect of ^{13}C implanted ions (6×10^{16} ions/cm^2, 100 or 180 keV) on the diffusion behaviour of SiC has been investigated at temperatures between 1600 and 1900°C. The implanted layer becomes amorphous after implantation and recrystallizes by epitaxy during the annealing treatments. The implanted C atoms in excess are trapped in the implantation profile zone and C diffusion towards the outer surface is enhanced with respect to inner C diffusion. It is suggested that this is related to microstructural modifications in the implanted layer. The atom diffusivity in the implanted layer is a function of the depth, and its values are much lower than those given in the literature for Si and/or C diffusion in SiC from film deposition techniques.

Der Einfluß implantierter ^{13}C Ionen (6×10^{16} Ionen/cm^2, 100 oder 180 keV) auf das Diffusionsverhalten von SiC wurde im Temperaturbereich zwischen 1600 und 1900°C untersucht. Die implantierte Schicht ist amorph und rekristallisiert epitaktisch bei nachfolgender Wärmebehandlung. Überschüssig implantierte C-Atome werden in der Implantations-Profilzone aufgenommen. Die Kohlenstoffdiffusion in Richtung nach außen verläuft im Vergleich zur Diffusion in das Innere des Materials schneller. Diese Beobachtung scheint mit Gefügeveränderungen der implantierten Schicht verknüpft zu sein. Die diffusivität der Atome innerhalb der implantierten Schicht hängt von der Tiefe ab. Die Werte des Diffusionskoeffizienten sind weitaus geringer als die, die in der Literatur angegeben werden für die Si- oder C-Diffusion in durch Abscheiden dünner Schichten hergestelltem SiC.

L'effet de l'implantation de ^{13}C sur le comportement diffusionnel de SiC a été étudié dans le domaine de températures 1600–1900°C; ce traceur a été introduit par implantation, sous 100 ou 180 keV et à une dose de 6×10^{16} ions/cm^2. La couche brute d'implantation est amorphe, puis, au cours de traitements thermiques, elle recristallise par épitaxie. Les atomes de C implantés sont piégés dans la zone du profil d'implantation et la diffusion du carbone vers la surface externe est accélérée par rapport à la diffusion vers le coeur du matériau. Cette observation semble liée aux modifications microstructurales dans la couche implantée. La diffusivité de ces atomes dans la couche implantée dépend de la profondeur et les valeurs des coefficients de diffusion sont plus faibles que celles données dans la littérature, pour la diffusion du carbone ou du silicium dans SiC, à partir de méthodes de films minces.

1 Introduction

For many years there has been great interest in ceramic materials such as silicon carbide or nitride for applications as structural materials, due to their good mechanical properties at high temperature and in aggressive atmospheres. So it is important to determine the thermal stability of such materials which depends, for a great part, on diffusion

* Present address: Institute of Corrosion and Protection of Metals, Academia Sinica, Shenyang, China.

Journal of the European Ceramic Society 0955-2219/93/$6.00 © 1993 Elsevier Science Publishers Ltd, England. Printed in Great Britain

processes. To date, results about self-diffusion in such materials are not numerous, and the objective, at the beginning of this work, was to determine self-diffusion coefficients in SiC in order to obtain a better understanding of its high-temperature behaviour in aggressive atmospheres.[1]

Ion implantation in the materials is an interesting method from both technological and fundamental aspects, for the surface property modification of materials (or interface property modification in the case of composites), and for solid-state atomic diffusion studies. With the implantation technique it is possible to study some diffusion systems that are difficult to address experimentally by other techniques. For instance, carbon diffusion in stoichiometric niobium carbide[2] was determined by such a method. Implantation is also a useful tool for studying diffusion of some elements which are not soluble in the substrate, for instance copper and silver in beryllium.[3] This technique also has the advantage of avoiding surface contamination during tracer introduction.

Obviously, tracer introduction in the crystalline substrate by implantation produces some structural defects (or an amorphization in the implanted layer) and a local variation of the chemical composition. This often induces a diffusion behaviour which differs from that observed in equilibrium processes. The study of the diffusion behaviour of implanted elements and of the structural changes in the implanted layer are therefore of great interest for a better understanding of these equilibrium and non-equilibrium processes.

So, in this investigation, the relation between the microstructural modifications due to implantation and the self-diffusion rates and mechanisms in SiC were examined.

2 Material and Experimental Methods

2.1 Material

Single crystals of SiC, provided by Lonza (Switzerland) and Sofrem (Péchiney Electrométallurgie, Aiguebelle, France), were obtained by the Acheson process. These single crystals are dense. The structure determination by X-ray diffraction (Laue technique and diffractometry on powder of single crystals) showed that the single crystals corresponded to α-SiC, with several polytypes in the same sample (6H, 4H and 15R being predominant).

Figure 1 shows the dislocation distribution on a (00·1) plane. This image was obtained by chemical etching in molten NaOH at 800°C for 90 s.[4] The dislocation distribution is not homogeneous.

Single crystals were oriented by the Laue method so that the large face of the samples was always parallel to the (00·1) plane. Then samples were carefully cut in order to obtain two faces parallel to the (00·1) and (00·$\bar{1}$) planes, respectively. Each face was diamond polished to 2 μm grit size. After polishing, the samples were cleaned, first in hydrofluoric acid (HF) in order to eliminate the thin silica surface film (SiO_2), then in acetone. Before implantation, samples were heat treated for 1 h at 1600°C in a graphite resistor furnace in 1 atm of pure argon (99·9995% purity) in order to recover the surface layers hardened by polishing.

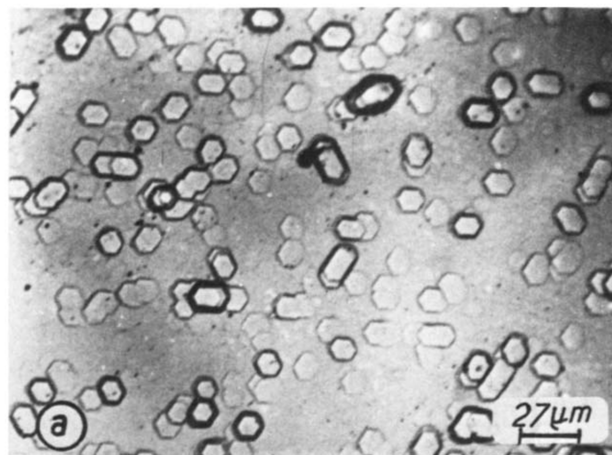

Fig. 1. Dislocation distribution on the (00·1) plane of α-SiC single crystals.

2.2 Implantation

Three series of implantations, whose characteristics are given in Table 1, were performed. The first and second series concern ^{13}C implantation made with different energy, 100 and 180 keV, respectively. As will be seen later, after such implantations and diffusion treatments, outward diffusion of implanted carbon was observed. In order to avoid or reduce this phenomenon, an attempt was made to introduce by implantation both carbon and silicon (^{13}C and ^{29}Si), to stabilize these elements as SiC in the substrate. The implantation energy difference for carbon and silicon was chosen in order to obtain the same position of the implanted peak in the substrate. In all cases the implantation dose was equal to 6×10^{16} ions/cm². Implantations were performed at room temperature. The flux was equal to $1{\cdot}24 \times 10^{17}$ ions/m² s in the experiments (implantation during ≈ 80 min), and the energy density equal to $1{\cdot}98 \times 10^{3}$

Table 1. Implantation conditions

	Implanted atoms	*Implantation dose (ions/cm²)*	*Energy, E (keV)*
Single implantation	^{13}C	6×10^{16}	100
	^{13}C	6×10^{16}	180
Double implantation	^{13}C	6×10^{16}	100
	^{29}Si	6×10^{16}	180

W/m^2. Hence it was calculated that the temperature increase must be lower than 80°C. In the experimental conditions of implantation, it can be assumed that the loss of matter by sputtering during implantation is negligible.[5]

For some samples (see later Berg–Barrett experiments and swelling measurements) half of the surface only was subjected to implantation. In addition, some other samples were implanted on the two surfaces in order to determine if the crystal orientation had an influence on the microstructural changes and on the diffusion behaviour.

After implantation, all samples were subjected to a recovery annealing in a graphite resistor furnace. The samples, surrounded by SiC grains in order to avoid vaporization at high temperature, were closed in a graphite crucible. The samples in the furnace were heated at 600°C/h in vacuum ($2{\cdot}6 \times 10^{-8}$ atm) up to 800°C, then argon was introduced (1 atm), again in order to avoid evaporation phenomena. Most of the recovery annealings were performed at 1600°C for 6 h, but some of them were made at lower temperatures in order to determine the evolution of the properties of the implanted surfaces during heating at various temperatures.

2.3 SIMS analyses

The evolution of the concentration profiles of implanted elements was analysed by secondary ion mass spectrometry (CAMECA IMS 3F). In order to avoid the charge accumulation, a thin gold layer (≈ 150 Å) was previously deposited on the SiC single crystals. The primary ions consisted either of Cs^+ or O_2^+ with an energy of 10 keV. The scanned area was equal to $250 \times 250\,\mu m^2$ with a probe diameter equal to 50 μm. The depth resolution is a few nanometres.

The experimental curves, element intensity versus sputtering time, were converted into curves of the evolution of the concentration versus the penetration depth. Taking into account the fact that the natural isotopic abundance of ^{13}C is equal to 1·107 wt% and that of ^{29}Si is 4·7 wt%, the implanted element concentration was calculated by doing the following intensity ratios:

$$I(^{13}C)/I(^{12}C) \quad \text{or} \quad I(^{13}C)/[I(^{12}C)+I(^{13}C)]$$
$$I(^{29}Si)/I(^{28}Si) \quad \text{or} \quad I(^{29}Si)/[I(^{28}Si)+I(^{29}Si)]$$

and using the following equation (written for the case of ^{13}C):

$$C(t_i) = \left[\frac{B(t_i)}{D(t_i)} - RS\right]R \qquad (1)$$

where $C(t_i)$ is the implanted ^{13}C concentration in the substrate for a sputtering time t_i; $B(t_i)$ is the ^{13}C intensity (^{13}C of the substrate + implanted ^{13}C) for a sputtering time t_i; $D(t_i)$ is the reference mass intensity ($^{12}C + {}^{13}C$) corresponding to the sputtering time t_i; RS is the value of the ratio of ^{13}C intensity to the reference mass intensity in a zone far from the implanted area (substrate core); and $R = a/RS$, where a is the natural abundance of ^{13}C in carbon.

The depth corresponding to the sputtering time t_i is calculated by the following equation:

$$x_i = \frac{D}{t_t}\,t \qquad (2)$$

where D is the crater depth measured by a TALYSTEP rugosimeter after the SIMS analysis and t_t is the whole sputtering time for the analysis. In the case of Si, $I(^{28}Si) + I(^{29}Si)$ was considered as reference mass intensity.

For the calculation of the depth x_i, the sputtering rate was considered as constant. This was verified by the linearity between the analysed depth and the electrical charge: the calculated sputtering rate for different sputtering times keeps a constant value.

2.4 Berg–Barrett technique

This technique was used in order to examine the structure evolution in the implanted layer during heat treatments. It is based on the fact that a plane subjected to a monochromatic X-ray beam gives X-ray diffraction if its position satisfies Bragg's condition. In this study, the Berg–Barrett tests were performed, with the CuK_α X-ray, on a sample whose surface was parallel to the (00·6) plane, the samples having been half-implanted (^{13}C, 100 keV, 6×10^{16} ions/cm^2). The topography contrast after implantation indicates the perturbations to which the implanted area has been submitted, and the contrast evolution during further treatments shows the evolution of the structure of this area. Two reflecting planes have been retained:

- The (10·$\underline{10}$) plane is in the Bragg position if the incident X-ray beam makes an angle equal to 6·43° with the sample surface. In such a case, due to the value of the mass absorption coefficient of the CuK_α X-ray in SiC (43·8 cm^2/g), the mean diffraction depth of the (10·$\underline{10}$) planes is equal to 8·06 μm. Thus the contrast will be mainly representative of unimplanted areas, i.e. of the SiC substrate.
- The (10·9) plane is in the Bragg position if the incident X-ray beam makes an angle equal to 0·7° with the sample surface. Then the mean diffraction depth of the (10·9) planes is equal to 0·887 μm and the contrast will be mainly representative of the implanted layer.

2.5 Microhardness and swelling

Vickers microhardness measurements were performed on implanted surfaces and after heat

treatments in order to obtain an idea of the plasticity evolution of the implanted zone.

The sample swelling related to the structure modifications due to implantation (defects creation and recovery) was determined by comparing the surface level of the two parts of half-implanted samples, after implantation and after recovery treatments. Such measurements were performed with a TALYSTEP profilometer, as for the determinations of the crater depth after SIMS analyses.

2.6 Other techniques

Samples were examined by scanning electronic microscopy. An attempt was made to obtain transverse thin foils of the implanted samples and to observe the microstructure of both the implanted and unimplanted areas.

Other techniques, such as X-ray diffraction, electronic microprobe analyses and X-ray photoelectron spectroscopy analyses (XPS), gave some more information.

3 Results

Figure 2 shows an example of carbon profile obtained on an as-implanted sample (denoted I in the following graphs and continuous line in Fig. 2) and after a stabilization annealing for 6 h at 1600°C (sample denoted S further on and dashed line in Fig. 2). These profiles have a Gaussian shape, as suggested by the LSS theory (of Lindhart, Scharff and Schiott). The area under the peak is in good agreement with the experimental dose. The difference between the depth of the peaks before and after the stabilization annealing is due to the recovery of the implanted zone structure during the annealing. The atom distribution was calculated by a model based on the Monte Carlo method,[6] and the calculated profiles fit the experimental ones well.

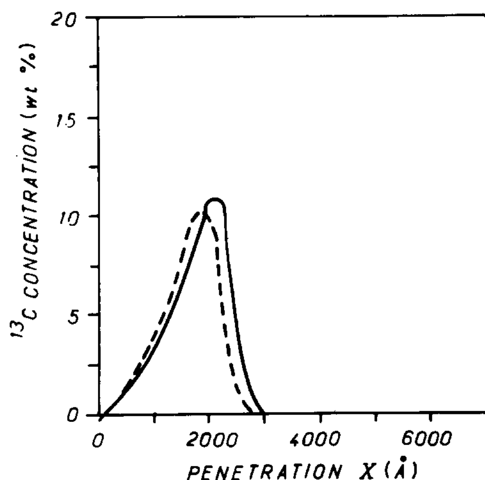

Fig. 2. ^{13}C concentration profile (——) after implantation (I) and (– – –) after a stabilization annealing (S) at 1600°C for 6 h. Implantation at 100 keV, 6×10^{16} ions/cm^2.

In the case of single implantation (^{13}C) at 100 keV, the peak depth is equal to 180 nm and the energy received by the implanted zone is equal to 6×10^{18} keV/cm^2. When carbon is implanted at 180 keV, the peak depth is equal to 290 nm and the energy received by the implanted zone is equal to $1{\cdot}08 \times 10^{19}$ keV/cm^2. In the case of double implantation, ^{13}C at 100 keV and ^{29}Si at 180 keV, the peak depth is equal to 180 nm for both C and Si, and the energy is equal to $1{\cdot}68 \times 10^{19}$ keV/cm^2. The energy received by the implanted zone is representative of the perturbation degree of this zone.

In studying the evolution of the profiles during diffusion heat treatments, and calculating a diffusion coefficient, the profile obtained after the stabilization treatment is taken as the initial profile.

3.1 Single implantation of ^{13}C at 100 or 180 keV

The evolution of ^{13}C profiles during diffusion annealings (denoted D) is shown in Figs 3–6. In Fig. 3 (I, 100 keV; S, 6 h at 1600°C; D at 1800°C for various durations) curves 1 and 2 correspond to

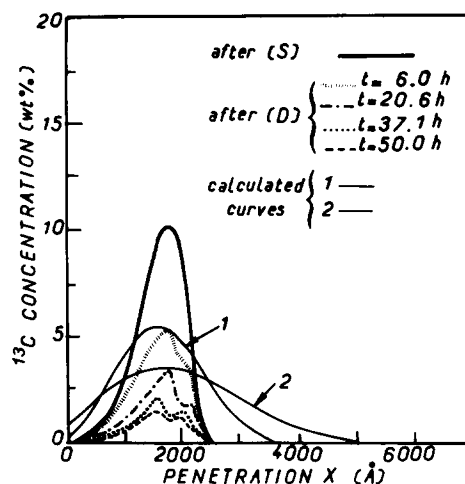

Fig. 3. ^{13}C concentration evolution versus SiC depth: I, 100 keV; S, 1600°C for 6 h; D (diffusion annealing), 1800°C for various times.

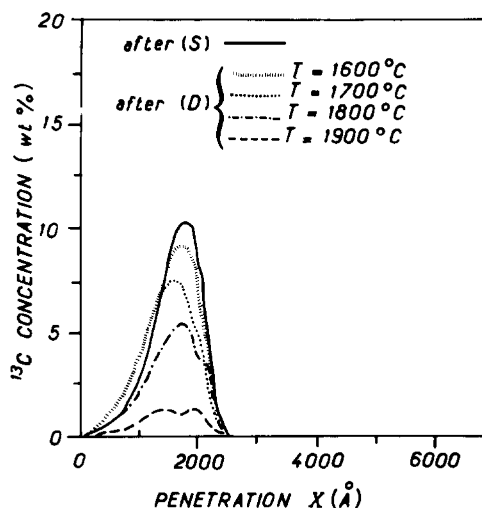

Fig. 4. ^{13}C concentration evolution versus SiC depth: I, 100 keV; S, 1600°C for 6 h; D, 6 h at various temperatures.

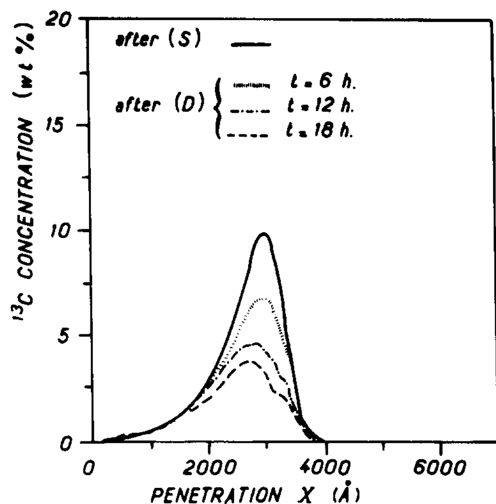

Fig. 5. ^{13}C concentration evolution versus SiC depth: I, 180 keV; S, 1600°C for 6 h; D, 1800°C for various times.

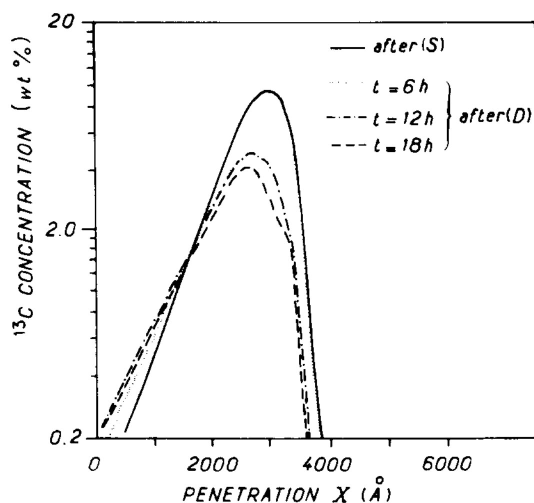

Fig. 6. ^{13}C concentration evolution versus SiC depth: semi-logarithmic plot of Fig. 5.

theoretical profiles calculated from the initial profile, by considering that the diffusion obeys the solution of Fick's law corresponding to an initial profile with a Gaussian shape,[7,8] and taking $t = 6$ h and $D = 10^{-16}$ cm^2/s for curve 1, and $t = 20{\cdot}6$ h and $D = 10^{-15}$ cm^2/s for curve 2. D values were fitted in order that the maximum of the calculated peak is superimposed on that of the experimental one. By comparing curves 1 and 2 to the other experimental curves, it clearly appears that this solution is not adequate.

All experimental curves look similar whatever the diffusion temperature and the implantation energy (Figs 4 and 5). This suggests that the diffusion behaviour of implanted atoms always obeys the same mechanism.

These profiles indicate that the implanted atoms do not diffuse towards the sample core (even if such curves are plotted in semi-logarithmic coordinates, as in Fig. 6, that offers the advantage of giving a better representation for low concentrations). No significant evolution of the profiles towards the inner part of the samples occurs, while it clearly appears that during diffusion treatments the implanted ^{13}C atoms diffuse outward.

With increasing annealing time or temperature, a trough between two bumps appears at the initial position of the maximum of the peak.

The ^{13}C concentration at the outer surface is equal to the natural abundance of ^{13}C (transparency of the surface) and the tracer loss increases with the annealing time or temperature.

The tracer loss during the diffusion annealings was calculated from the changes in area under the concentration profiles. The results are shown in Fig. 7(a) and (b) as a function of the annealing time and temperature, respectively, for the carbon implantation at 100 and 180 keV. For a given temperature (Fig. 7(a)) the tracer loss increases with time (according to a law which is not parabolic), and for a given time (Fig. 7(b)) the tracer loss increases with temperature. The tracer loss is greater when the implantation is performed at 100 keV than at 180 keV, all other conditions being equal.

By considering, after the diffusion annealings, the SIMS signal intensities on 28, 12 and 13 masses (silicon and carbon in the substrate, and implanted carbon, respectively; Fig. 8), a ^{28}Si decrease and an increase of both ^{12}C and $^{12+13}$C clearly appear at the

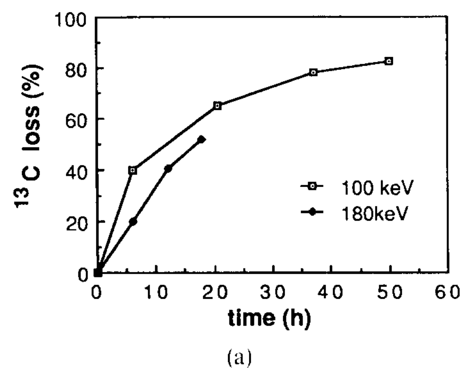

(a)

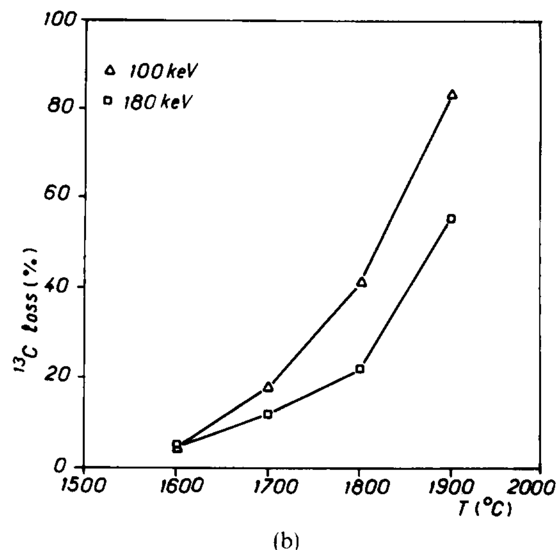

(b)

Fig. 7. ^{13}C loss versus (a) time during diffusion annealing at 1800°C and (b) the diffusion temperature for 6-h annealing.

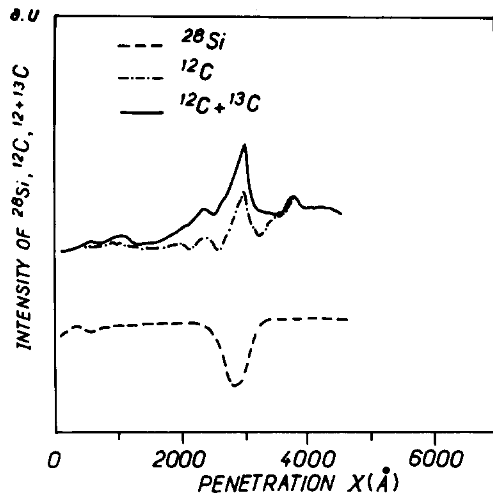

Fig. 8. SIMS signal intensities of ^{28}Si, ^{12}C and ^{12}C + ^{13}C versus depth after a diffusion annealing for 6 h at 1800°C. I, 180 keV; S, 1600°C for 6 h.

position of the maximum of the ^{13}C implanted peak. The increase in $^{12+13}$C justifies the ^{13}C trough between two bumps previously observed in Figs 3–5, where the ordinate corresponds to the ratio ^{13}C/$^{12+13}$C. With the diffusion annealing going on, the $^{12+13}$C peak and the ^{28}Si trough increase, at least up to 1800°C. This suggests the formation, during such treatments, of a layer enriched in carbon (gathered or precipitated). This also indicates that a part of the carbon of the substrate (^{12}C) has diffused in the carbon-enriched layer and has exchanged with ^{13}C (these atoms substituting ^{12}C atoms of the substrate lattice). For a diffusion annealing at 1900°C for 6 h these variations disappear.

3.2 Implantations of both ^{29}Si and ^{13}C

Figure 9 shows the evolution of the ^{29}Si and ^{13}C concentration profiles for different diffusion annealing temperatures. During these diffusion treatments the ^{13}C atoms again diffuse towards the outer surface, as for single implantations. They are not stabilized by the implanted Si atoms, as was originally hoped: it seems that the ^{29}Si and ^{13}C atoms have not built up a SiC network. In the inner part of the implanted zone there is no carbon diffusion because carbon is trapped, as for samples singly implanted.

^{29}Si atom diffusion is negligible both towards the outer surface and towards the inner parts of the samples.

The signal intensities on 28, 12, (12 + 13) and (28 + 29) masses are shown in Fig. 10. After implantation, an excess of carbon appears on the curve of (12 + 13) masses corresponding to the implanted carbon (≈10%). After a diffusion treatment of 6 h at 1600°C, the excess in (12 + 13) carbon has disappeared, when most of the ^{13}C remains in the implanted zone (cf. Fig. 9). This indicates that a ^{12}C and ^{13}C mixing has occurred during implan-

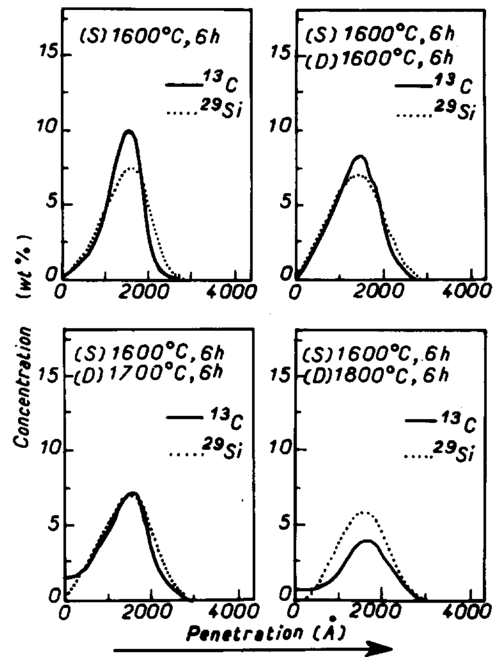

Fig. 9. ^{13}C and ^{29}Si concentration evolution versus SiC depth after diffusion annealing for 6 h at various temperatures. Double implantation: ^{13}C implanted at 100 keV and ^{29}Si implanted at 180 keV. S, 1600°C for 6 h in all cases.

tation, and that progressively there is a carbon balancing. Moreover, at the outer surface, a carbon increase and a silicon decrease is noted. That corresponds to a decomposition of the material. For instance, a diffusion annealing for 6 h at 1700 and 1800°C induces a SiC decomposition up to 40 and 140 nm, respectively. By comparison, with the case of single implantations, it can be suggested that the larger implantation energy for double implantation

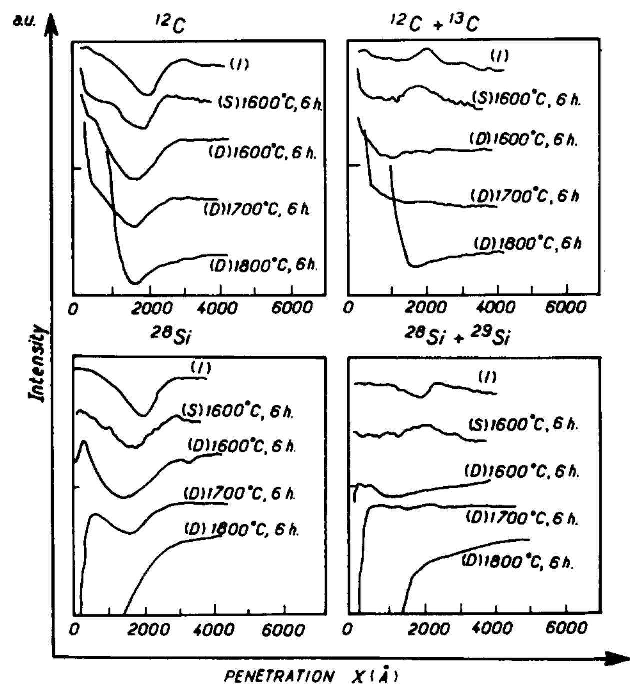

Fig. 10. SIMS signal intensities versus depth after a double implantation (^{13}C, 100 keV, and ^{29}Si, 180 keV) and various annealings.

induces a change in the thermal stability of SiC and that the restoration during the stabilization annealing has not been sufficient.

4 Discussion

4.1 Diffusivity of ^{13}C in the implanted layer

As the solution of Fick's law used is not adequate (see Fig. 3), and as an asymmetry clearly appears in the carbon profiles after diffusion treatments, another attempt was made to evaluate the carbon diffusivity in the SiC implanted layers whose structure is modified during the heat treatments. For this calculation it was assumed that a stationary diffusion regime is established, because:

(i) Towards the outer surface it is observed that the carbon concentration profiles are not modified as diffusion annealings are going on (see Fig. 6), even though the tracer loss is significant. This suggests that the ^{13}C concentration is relatively independent of time and temperature for $x < 120$ nm. This concentration follows an exponential variation between $x = 0$ and $x = 120$ nm, and can be expressed according to $C(x) = a10^{bx}$, a and b being constants.

(ii) For relatively short diffusion annealings (for instance 10 h at 1800°C) the tracer loss rate can be considered as constant (see Fig. 7(a)).

(iii) Moreover, this stationary diffusion regime can be justified by the fact that the carbon-enriched layer can provide sufficient carbon atoms to maintain a constant flow.

Considering the first Fick's law:

$$J = -D\frac{dC(x)}{dx} \tag{3}$$

where J, the ^{13}C atom flow in atom/cm^2 s, is a constant and can be calculated from the tracer loss during the diffusion annealings; D, in cm^2/s, is the ^{13}C diffusion coefficient in the implanted zone; and $dC(x)/dx$ is the ^{13}C concentration gradient.

By derivation of $C(x) = a10^{bx}$, it becomes

$$dC(x)/dx = bC(x) \quad \text{and} \quad D = -J/bC(x) \tag{4}$$

with J/b = constant.

This expression indicates that the ^{13}C diffusion coefficients in the implanted layer depend on the tracer concentration, i.e. on the depth. The constant depends on the diffusion annealing temperature and time. It appears that the greater the carbon concentration, the smaller the diffusion coefficient. The carbon diffusion coefficient increases when the distance from the outer surface decreases.

The values of the carbon diffusion coefficients are

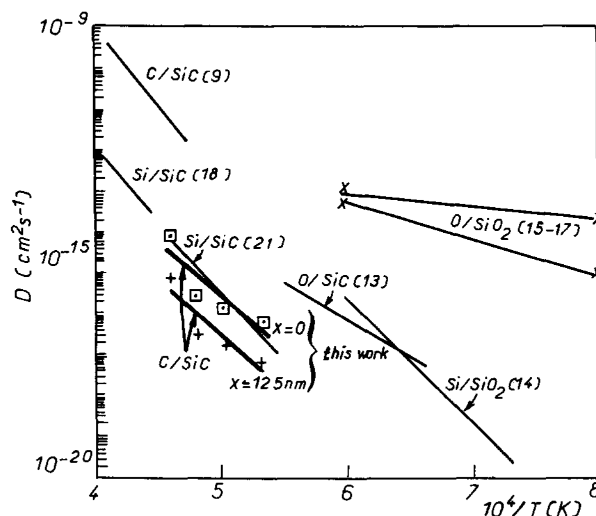

Fig. 11. Arrhenius plot of diffusion coefficients in SiC and SiO_2. Present results (^{13}C implanted at 180 keV in SiC) and literature data.

given in Fig. 11 for two depths: $x = 0$ (outer surface) and $x = 125$ nm (annealing time = 6 h and implantation energy = 180 keV). It appears that the carbon diffusion coefficients in the implanted layer are thermally activated. The activation energy and the values of the carbon diffusion coefficients obtained in this study are smaller than the values given by Hong,[9] the only data relative to carbon diffusion in SiC but determined by another method (tracer film deposition).

The asymmetry of the carbon profiles reflects the different structure of two regions in the implanted material: an amorphous or nanocrystalline region towards the outer surface, and a perfectly crystalline region after the implantation peak. Then it could be expected to obtain diffusion coefficients higher than those obtained by Hong. As the diffusion coefficients are about four orders of magnitude lower than the values of Hong, it can be suggested that a different diffusion mechanism is involved for implanted atoms.

4.2 Diffusion mechanism of implanted atoms

As indicated previously (Fig. 8), due to the excess of carbon, ^{12}C and ^{13}C form an inner layer enriched in carbon. This layer probably corresponds to a second phase precipitation which modifies the kinetics of carbon diffusion. Two steps have then to be considered: a first one which corresponds to the dissolution of the second phase, and a second step corresponding to the diffusion of carbon. On the basis of Hong's results, it can be suggested that the diffusion-controlled step is the fastest, which indicates that the dissolution step is slow. So, in the present case, the diffusivity of implanted atoms is controlled by their delivery from the carbon-enriched layer. This would explain the fact that D varies with the depth and increases when the

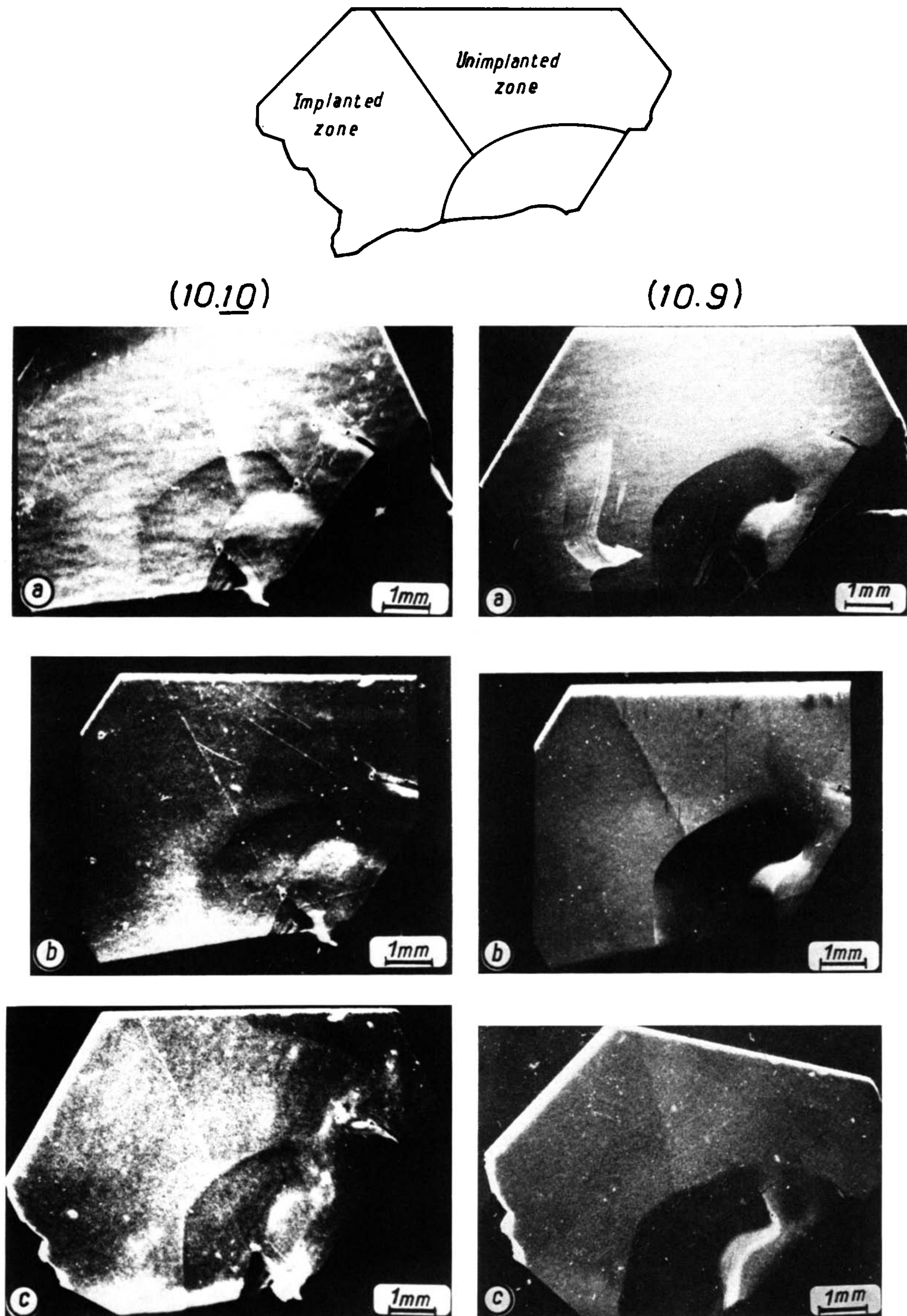

Fig. 12. Berg–Barrett topography on (10·1̲0̲) on the left and (10·9) on the right. (a) Before implantation; (b) after ^{13}C implantation (100 keV); (c) after implantation and stabilization annealing for 6 h at 1600°C. Samples implanted on half of the surface, as shown in the scheme.

distance from the outer surface decreases. Moreover, due to microstructural modifications of the implanted zone, carbon diffusion occurs preferentially towards the outer surface. This surface acts as a sink for ^{13}C, due to the natural carbon atmosphere in the furnace, inducing an isotopic exchange.

So the measurement of carbon diffusion coefficients in SiC by an implantation method leads to diffusion values which are not representative of lattice self-diffusion coefficients, on account of the structural evolution of the implanted layer and of trapping phenomena. It must be noted that this observation is not always made: in materials such as Cr_2O_3,[10] NiO,[8] TiN[11] and Si,[12] implantation, film deposition or exchange methods lead to similar values of the self-diffusion coefficients and an outward diffusion of the implanted element is not observed.

As with Hong,[9] it is observed that silicon diffusion is slower than carbon diffusion.

According to these results, it is interesting, in order to obtain a better understanding of the oxidation behaviour of SiC, to compare the order of magnitude of diffusion coefficients in SiC and SiO_2. Extrapolated diffusion data in the literature[1,13–18] are plotted in Fig. 11, with the present results and those of Hong concerning carbon diffusion in SiC. By comparing all these data, the following sequence can be proposed:

$$D^{Si}_{SiC} < D^{C}_{SiC}, D^{Si}_{SiO_2}, D^{O}_{SiC} < D^{O}_{SiO_2} < D^{C}_{SiO_2}$$

4.3 Amorphization of the implanted layer

According to the Spitznagel criterion,[19] it is possible to calculate the critical energy necessary to induce an amorphization of the implanted surface at $x = 0$, and at the depth of the maximum of the peak. At 100 or 180 keV the ^{13}C dose necessary to induce an amorphization of the surface is equal to $3{\cdot}3 \times 10^{15}$ ions/cm^2 or $6{\cdot}0 \times 10^{15}$ ions/cm^2, respectively. The implantation dose in this study is greater (one order of magnitude) than these critical doses. So it is reasonable to estimate that, in all the implantation series, the implanted zone becomes amorphous. This was also suggested by preliminary observations of transverse thin foils by TEM, whose interpretation needs further studies.

The Berg–Barrett experiments confirmed this assumption. A sample was implanted in ^{13}C at 100 keV on half of its surface. Two planes, $(10{\cdot}\underline{10})$ and (10·9), were studied. The topography of the whole surface was examined before and after implantation (Fig. 12(a) and (b)), and after a stabilization annealing for 6 h at 1600°C (Fig. 12(c)).

Before implantation, the X-ray image for the two planes does not show any difference. After implantation, a contrast is observed between the two parts of the sample when the topography is performed on the (10·9) plane: the X-ray diffraction in the implanted zone is smaller. The topography on the $(10{\cdot}\underline{10})$ plane does not show any contrast. The diffraction on the (10·9) plane is representative of a perturbation in the implanted zone. After the stabilization annealing, the contrast has largely decreased, indicating that restoration occurred during this annealing but was not complete.

Hardness tests are also in agreement with the idea of an amorphization of the implanted zone. The hardness measurements were made with a load of 100 g, which leads to an imprint of $\approx 1{\cdot}2\,\mu$m depth. As the implanted zone depth is lower than $0{\cdot}4\,\mu$m, the measured value corresponds to the response of both the substrate and the implanted zone. The measured values of Vickers hardness are always about $\mu H_{v_{100}} = 3000$, whatever the sample treatment. However, the evolution of the morphology around the imprint indicated that a plasticity change occurred during implantation. On unimplanted samples the imprints are always surrounded by radial cracks, while such cracks are not observed after implantation. They again appear after annealings. This indicates that implantation induces an increase of the plasticity, and that the microstructural modifications related to the restoration which occur during further annealings decrease the SiC plasticity. These plasticity modifications are related to the defect created by the implanted atoms and their progressive elimination.

Two other observations support the formation of an amorphous implanted zone, i.e. the colour change of the samples and their swelling:

(i) For SiC the energy gap of the forbidden band is approximately equal to 3 eV. Thus all visible radiations are transmitted and the material is colourless. After implantation, the SiC single crystals become dark brown. This colour progressively disappears during further annealings.

(ii) The measurements of the swelling were made on samples half-implanted by comparison of the surface level with a rugosimeter. The swelling is characterized by the height difference (denoted H) between the two zones of the sample. Figure 13 shows that H is significant after implantation and decreases with further annealings. After implantation, the swelling is equal to 35 nm. This is a minimal value due to the fact that the sputtering during implantation is not really equal to zero.[5] By considering that the implanted scale thickness is equal to 250 nm (in the case of the sample corresponding to Fig. 13), and that the introduced carbon

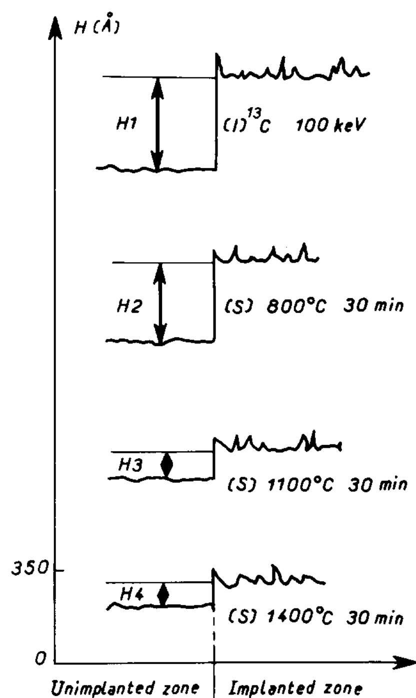

Fig. 13. Swelling of the implanted surfaces.

atoms (6×10^{16} ions/cm^2) induce a thickness increase equal to 7 nm, it can be said that about 80% of the swelling is due to the creation of defects.

All these considerations suggest that the implantation induces the formation of an amorphous or heavily disordered zone.

4.4 Structural restoration during annealings

The structural recrystallization of an amorphous scale formed by implantation can occur according to two possibilities, either nucleation and growth or epitaxy.[20] According to the experimental results, it can be said that the recrystallization occurs by epitaxy on the substrate. Indeed, the Berg–Barrett images (Fig. 12) show that the amorphous layer recrystallizes with the same orientation as that of the substrate. In the case of double implantation (^{13}C and ^{29}Si) hexagonal sub-boundaries appear in the implanted layer which correspond to the crystallographic characteristics of the substrate.

The restoration process depends on the implantation dose and on the annealing time and temperature.

In the case of ^{13}C implantation at 100 keV, the surface morphology is not affected by the implantation, and it does not evolve during further annealings. However, in the case of implantation at 180 keV, if nothing is observed directly after implantation, cracks are evidenced after the stabilization annealing and they subsist during further heat treatments. In the case of double implantation, most of the surface is not affected after implantation, except some zones where little cracks

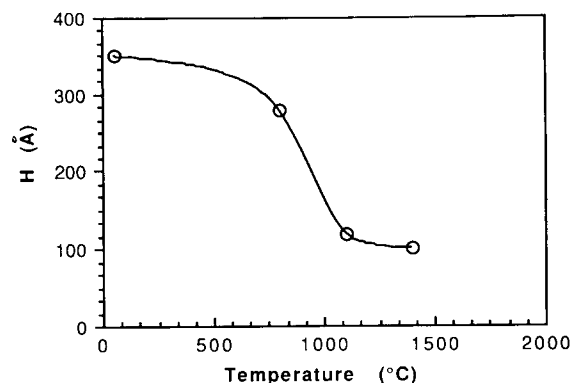

Fig. 14. Swelling evolution versus the temperature of the stabilization annealing (30 min) after ^{13}C implantation (100 keV).

are observed. These cracks appear on the whole surface after a stabilization annealing for 6 h at 1600°C and further heat treatments do not modify this morphology. The crack formation must be related to the thickness of the amorphous zone which increases with the implantation energy.

The colour and the swelling evolutions during the annealings indicate that most of the point defects are eliminated by heat treatments between 800 and 1100°C, as shown by Fig. 14. However, this elimination of the point defects in this temperature range is not complete, as evidenced by the particular behaviour of the implanted atoms, at higher annealing temperatures.

4.5 Implanted layer decomposition

As shown in Fig. 10, after a double implantation and annealing at a high temperature (1700–1800°C), SIMS analyses show, at the surface, an increase in carbon concentration associated with a decrease in silicon concentration which correspond to SiC decomposition. For instance, an annealing for 6 h at 1700°C and at 1800°C induces a SiC decomposition up to $\approx$40 and 140 nm, respectively. The great absorbed energy, when compared to single implantation cases, induces a modification of the thermal stability of SiC and the stabilization annealing at 1600°C (6 h) is insufficient to induce a complete restoration. The expected decomposition mechanism is the following: it begins by a preferential loss of silicon, which induces the formation of a carbon-enriched layer at the surface. When the decomposition front line reaches the unimplanted zone, then the silicon loss stops and a carbon loss occurs so that the surface becomes again stoichiometric, as shown by Fig. 15.

The influence of the stabilization annealing temperature on the decomposition of this material is important. It was observed that the conditions of the stabilization annealing can modify the surface morphology. For diffusion annealings up to 1600°C the surface morphology only shows cracks and does not depend on the stabilization annealing tempera-

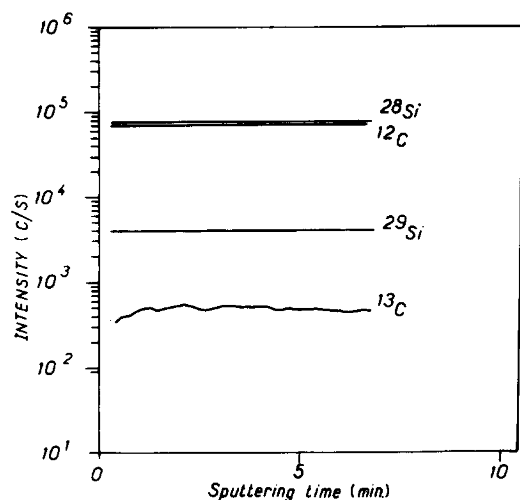

Fig. 15. SIMS signal intensities versus sputtering time (i.e. depth) on a SiC sample implanted in ^{13}C (100 keV) then stabilized firstly for 6 h at 1400°C then for 4 h at 1800°C.

ture. However, for diffusion treatments at 1700–1900°C the surface morphology differs according to the stabilization annealing temperature:

(i) If the stabilization annealing is performed at 1400°C, further diffusion treatments at 1700–1900°C lead to the surface morphology shown in Fig. 16. Simultaneously, it appears that the implanted layer has disappeared.
(ii) If the stabilization annealing is performed at 1600°C, a following diffusion treatment at 1700–1900°C does not induce such a decomposition.

Stabilization annealings at 1600°C induce a greater stability to the implanted layer than annealings at 1400°C. This indicates that the restoration phenomena depend on the temperature and that the restoration and the decomposition of the material are two competitive phenomena.

5 Conclusions

The study of the diffusion behaviour of carbon implanted ions in SiC single crystals was performed in the temperature range 1600–1900°C. Several series of implantations were chosen with the hope of stabilizing implanted atoms as a SiC compound. It appears that:

(i) The implanted atoms always diffuse towards the outer surface, probably on account of microstructural modifications of the implanted layer and of the sink effect played by the outer surface.
(ii) In the deepest parts of the implanted zone, the implanted atoms are trapped. At the position of the maximum of the ^{13}C concentration profile peak, a carbon-enriched layer

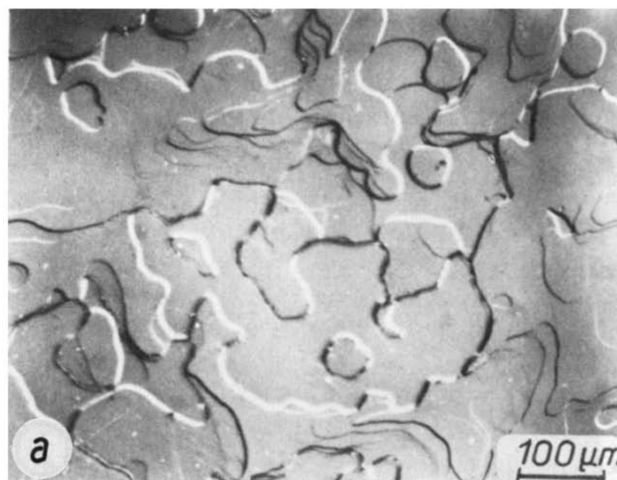

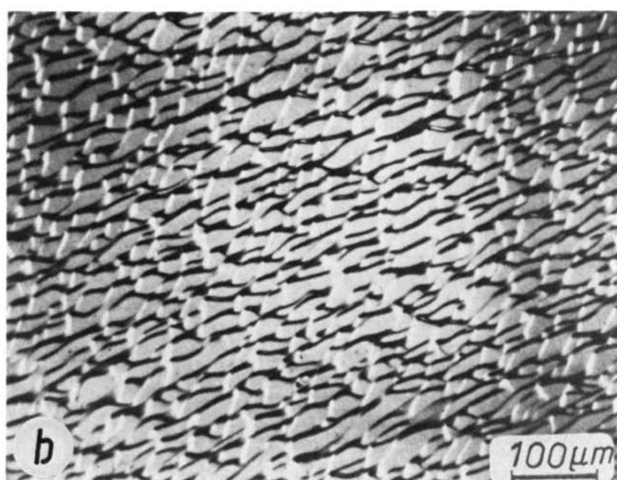

Fig. 16. α-SiC surface morphology after double implantation (^{13}C, 100 keV, and ^{29}Si, 180 keV), stabilization annealing for 6 h at 1400°C and a diffusion annealing for 4 h at (a) 1800°C and (b) 1900°C.

appears. This layer progressively disappears during further annealings.
(iii) In the case of the single implantations, the diffusion coefficients of ^{13}C atoms in the implanted layer are a function of the depth (or of the concentration): their values increase towards the outer surface. Both the activation energy and the diffusion coefficient values are significantly lower than that given in the literature for the carbon self-diffusion in SiC from a film deposition technique. This probably reflects a control of the diffusivity by the carbon delivery from the carbon-enriched layer. Thus the diffusion behaviour of these implanted atoms is not representative of the lattice self-diffusion. ^{29}Si still diffuses slower than ^{13}C does.
(iv) The implanted layer becomes amorphous or heavily disordered after the implantations, and it recrystallizes by epitaxy during the annealing treatments. An important structure recovery has been observed between 800 and 1100°C, but the structure is still per-

turbed at temperatures for which carbon diffusion begins.

(v) $^{13}C + ^{29}Si$ implantation does not allow a better restoration of the structure and induces a sample surface decomposition above 1700°C.

In the case of this study the implantation technique was not successful as a method for determining the self-diffusion coefficients as originally intended.

Acknowledgements

The authors are grateful to M. Backhaüs-Ricoult, J. Deschamps, M. Miloche and C. Waldburger of Laboratoire de Physique des Matériaux, CNRS Bellevue, for their help in the use of various techniques.

References

1. Li, J., Huntz, A. M. & Eveno, P., *Werkstoffe und Korr.*, **41** (1990) 716–25, and Li, J., Doctoral thesis, University Paris XI, Orsay, France, 1990.
2. Geerk, J. & Langguth, K. G., *Solid State Commun.*, **23** (1977) 83–7.
3. Myers, S. M. & Langley, R. A., *J. Appl. Phys.*, **46** (1975) 1034–42.
4. Brander, R. W. & Sutton, R. P., *Brit. J. Appl. Phys.*, **2** (1969) 309–18.
5. Roberts, S. G. & Page, T. F., *J. Mat. Sci.*, **21** (1986) 457–68.
6. Ziegler, J. F., Biersack, J. P. & Littmark, U., *The Stopping and Range of Ions in Solids, I and II.* Pergamon Press, Oxford, 1986.
7. Schimko, R., Schwarz, G. & Rogge, K., *Phys. State Sol. (a)*, **28** (1975) K163–K166.
8. Meyer, M., Barbezat, S., El-Houch, C. & Talon, R., *J. de Physique*, **41** (1980) C327–C330.
9. Hong, J. D., PhD thesis, North Carolina State University, USA, 1978.
10. Sabioni, A. C. S., Doctoral thesis, University Paris XI, Orsay, France, 1990 and Sabioni, A. C. S. *et al.*, *Phil. Mag. A.*, **66** (1992) 333–74.
11. Anglezio-Abautret, F., Doctoral thesis, University Paris VI, 1990, and Abautret, F. & Eveno, P., *Rev. Phys. Appl.*, **25** (1990) 1113–19.
12. Demond, F. J., Kalbitzer, S., Mannsperger, H. & Damjantschitsch, H., *Phys. Letters*, **93A** (1983) 503–6.
13. Waldburger, C., Meyer, M. & Eveno, P., In *Reactivity of Solids*. Mat. Sci. Monograph, Vol. **28B**, ed. P. Barret Elsevier, Amsterdam, 1985, p. 445.
14. Brebec, G., Seguin, R., Sella, C., Bevenot, J. & Martin, J. C., *Acta Met.*, **28** (1979) 327–33.
15. Sucov, E. W., *J. Am. Ceram. Soc.*, **46** (1963) 14–20.
16. Haul, R. & Dumbgen, G., *Z. Elektrochem.*, **66** (1962) 636–41.
17. Mueklenbachs, K. & Schaeffer, H. A., *Can. Mineralogist*, **15** (1977) 179–84.
18. Hong, J. D., Davis, R. F. & Newbury, D. E., *J. Mat. Sci.*, **16** (1981) 2485–94.
19. Spitznagel, J. A., Wood, S., Choyke, W. J. & Doyle, N. J., *Nucl. Instr. Meth.*, **B16** (1986) 237–43.
20. Olson, G. L. & Roth, J. A., *Mat. Sci. Rep.*, **3** (1988) 1–78.
21. Waldburger, C. & Eveno, P., 1991, pers. comm.